acta physica slovaca vol. 55 No. 3, 305 – 313 **June 2005**

FORMATION AND ELECTRICAL CHARACTERISTICS OF SILICON DIOXIDE LAYERS BY USE OF NITRIC ACID OXIDATION METHOD[1]

S. Imai,[a,2] **M. Takahashi**[b], **K. Matsuba**[b], **Asuha**[b], **Y. Ishikawa**[b], **Hikaru Kobayashi**[b]
[a] *System Solutions Planning Department, Electronic Components & Devices, Sharp Corporation, 2613-1, Ichinomoto-cho, Tenri, Nara 632-8567, Japan*
[b] *Institute of Scientific and Industrial Research, Osaka University, and CREST, Japan Science and Technology Organization, 8-1 Mohogaoka, Ibaraki, Osaka 567-0047, Japan*

Received 11 February 2005, accepted 25 April 2005

SiO_2/Si structure can be formed at low temperatures by use of nitric acid (HNO_3) oxidation of Si (NAOS) method. When Si wafers are immersed in $\sim$ 40 wt% HNO_3 solutions at 108°C, $\sim$ 1 nm SiO_2 layers are formed. The subsequent immersion in 68 wt% HNO3 (i.e., azeotropic mixture of HNO3 with water) at 121°C increases the SiO_2 thickness. The 3.5 nm-thick SiO_2 layers produced by this two-step NAOS method possess a considerably low leakage current density (e.g., 1×10^2 A/cmi^2 at the forward gate bias, V_G, of 1.5 V), in spite of the low temperature oxidation, and further decreased (e.g., 8×10^4 A/cm^2 at $V_G = 1.5$ V) by post-metallization annealing at 250°C in hydrogen atmosphere. In order to increase the SiO_2 thickness, a bias voltage is applied during the NAOS method. When 10 V is applied to Si with respect to a Pt counter electrode both immersed in 1 M HNO_3 solutions at 25°C, SiO_2 layers with 8 nm thickness can be formed for 1 h.

PACS: 85.40.Hp, 73.40.Qv, 81.60.Cp

1 Introduction

Gate oxide (SiO_2) layers in thin film transistors (TFT) are currently formed by the chemical vapor deposition (CVD) method using tetraethoxylorthosilicate (TEOS). Because of a high leakage current characteristic of the TEOS SiO_2 layers, a large thickness of $\sim$100 nm is necessary, which increases a threshold voltage and thus increases power consumption. The TEOS SiO_2 layers should be deposited at temperatures above $\sim$500 °C in order to avoid inclusion of carbon species which seriously degrades the SiO_2characteristics, e.g., an increase in the leakage current density [1, 2]. The high temperature deposition makes it impossible to use organic substrates such as polyethyleneterephthalete (PET). Low temperature deposition methods for the formation of SiO_2 layers have been proposed, e.g., plasma-enhanced CVD [3] , radical shower CVD [4] ,

[1] Presented at SSSI-IV (Solid State Surfaces and Interfaces IV) Conference, Smolenice, Slovakia, 8–11 Nov. 2004.
[2] E-mail address: imai.shigeki@sharp.co.jp

TEOS/ozone CVD [5], etc. However, SiO_2 layers formed by the deposition methods have high leakage current densities and poor interfacial characteristics.

We have recently developed a low temperature oxidation method by use of nitric acid (HNO_3), i.e., nitric acid oxidation of silicon (NAOS) method [6–10]. In cases where Si wafers were immersed in an azeotropic mixture of $HNO_3$and water (i.e., 68 wt % HNO_3), ultrathin (i.e., 1.4 nm) SiO_2 layers were formed and their leakage current density (e.g., $\sim$1 A/cm^2 at the forward gate bias, V_G, of 1 V) was as low as those for thermal oxide layers grown above 800 °C [11–13]. After post-metalization annealing (PMA) treatment in hydrogen at 200 °C, the leakage current density was further decreased (e.g., 0.4 A/cm^2 at V_G=1 V) [6, 9].

In the present study, we have developed the following two methods for the low temperature formation of thicker SiO_2 layers; 1) two-step NAOS method, and 2) bias-assisted NAOS method.

2 Experiments

Metal-oxide-semiconductor (MOS) diodes were fabricated from phosphorus-doped n-type Si(100) wafers with a $\sim$10 Ω cm resistivity. The Si wafers were cleaned using the RCA method [14], followed by etching with dilute hydrofluoric acid. For the formation of relatively thick SiO_2 layers using the NAOS method at zero bias, Si wafers were immersed in 40 wt % HNO_3 aqueous solutions at the boiling temperatures of 108 °C. Then, the specimens were immersed in 68 wt % HNO_3 solutions, i.e., the azeotropic mixture of HNO_3 with water, at the boiling temperature of 121°C.

For the bias-assisted NAOS method, ohmic contact was achieved by the deposition of an aluminum film on the upper part of the front Si surface. Then, the lower part of the Si wafer, and counter and reference platinum electrodes were immersed in 1 M HNO_3 solutions at 25 °C and a bias voltage ranging between 5 and 20 V was applied to the Si electrode with respect to the reference electrode. In some cases, post-oxidation anneal (POA) was performed at 600 °C in nitrogen for1 h. Aluminum (Al) dots of 0.3 mm diameter were formed by means of the thermal evaporation method, resulting in $<$Al/SiO_2/Si(100)$>$ MOS structure. For some specimens, post-metallization anneal (PMA) was carried out at 200 or 250 °C in 5 % hydrogen-containing nitrogen atmosphere for 1 h.

The thickness of the SiO_2 layers was estimated from x-ray photoelectron spectroscopy (XPS) and ellipsometry measurements using a VG SCIENTIFIC Escalab 220i-XL spectrometer with a monochromatic Al Kα radiation source and a Sopra GES-5 ellipsometer, respectively. Vibrational spectra of the SiO_2 layers were recorded with the incident angle of 65°using a Nicolet Nexus 370S Fourier transformed infrared (FT-IR) transmission spectrometer. Current-voltage (I-V) characteristics were measured with an HP 4140B picoammeter. Capacitance-voltage (C-V) curves were recorded at 100 kHz using an HP 4192 A impedance analyzer.

3 Results and Discussion

Figure 1 shows XPS spectra in the Si 2p region for the SiO_2/Si(100) specimens formed by the NAOS method at zero bias. Doublet peaks were due to Si $2p_{3/2}$ and $Si_{1/2}$ levels of the Si substrate, and a broad peak in the higher energy side was due to the SiO_2 layer. After the immersion of Si in the 40 wt % HNO_3 solutions for 10 min, a peak due to an SiO_2 layer

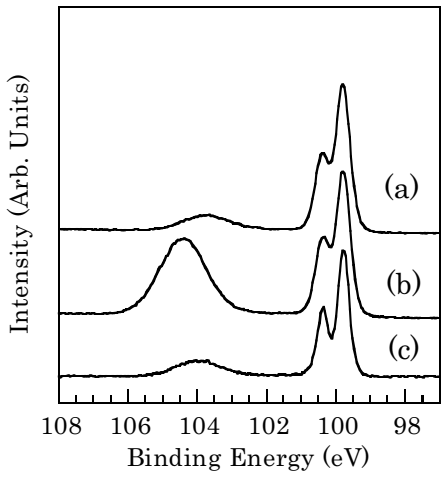

Fig. 1. XPS spectra in the Si 2p region for the SiO_2/Si structure formed by the immersion in the following HNO_3 aqueous solutions at the boiling temperatures: a) 40 wt % HNO_3 for 10 min; b) 40 wt % HNO_3 for 10 min and 68 wt % HNO_3 for 2 h; c) 68 wt % HNO_3 for 2 h.

was observed only with a weak intensity (spectrum a). Prolonged immersion in the 40 wt% HNO_3solution did not increase the intensity of the SiO_2 peak. When this specimen with the ultrathin SiO_2 layer was immersed in the 68 wt% HNO_3 solution at 121 °C, on the other hand, the intensity of the peak due to SiO_2 markedly increased (spectrum b).

The thickness of the SiO_2 layers can be estimated from the ratio between the SiO_2 and substrate Si 2p peak area intensities [15, 16]. In the estimation, 3.2 nm was adopted as the mean free path of photoelectrons in SiO_2. Using this mean free path value, XPS analysis gives the same thickness values for the SiO_2 layers thicker than 4 nm (not shown in the figure) as those given by ellipsometry measurements. The thickness of the SiO_2 layers formed with 40 wt % HNO_3 was estimated to be 1.1 nm (spectrum a), and it increased to 3.5 nm after the immersion in 68 wt % HNO_3 for 2 h (spectrum b). In cases where the Si(100) wafers were immersed in the 68 wt % HNO_3 solution at 121 °C from the first, the Si oxidation stopped at the SiO_2 thickness of 1.4 nm (spectrum c).

Figure 2 shows FT-IR spectra in the Si-O-Si asymmetric vibrational region for the NAOS SiO_2/Si(100) specimens. Peaks at 1050 and ∼1230 cm^{-1} are attributable to TO and LO phonons, respectively, for SiO_2 [17–20]. The vibrational frequency of TO phonons,υ_{T0} , and that of LO phonons, υ_{L0}, are given by [17]

$$\upsilon_{TO} = \frac{1}{2\pi}\sqrt{2[\alpha \sin^2(\theta/2) + \beta \cos^2(\theta/2)]/m}, \tag{1}$$

$$\upsilon_{LO} = \frac{1}{2\pi}\sqrt{2[\alpha \sin^2(\theta/2) + \beta \cos^2(\theta/2)]/m + Z^2\rho/\varepsilon_\infty (2m + M)]/m}, \tag{2}$$

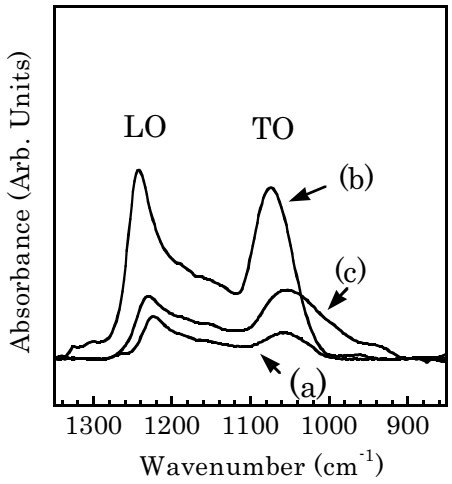

Fig. 2. FT-IR spectra in the Si-O-Si asymmetric stretching vibrational region for the SiO_2/Si structure formed by the immersion in the following HNO_3 aqueous solutions at the boiling temperatures: a) 40 wt % HNO_3 for 10 min; b) 40 wt % HNO_3 for 10 min and 68 wt % HNO_3 for 2 h; c) 68 wt % HNO_3 for 2 h.

where α and β are the central and noncentral force constants, respectively, θ is the Si-O-Si bridging bond angle, *m* and *M* are the masses of oxygen and Si atoms, respectively, ε_∞ is the permittivity at the infinite frequency, *Z* is the electrical charge related to the movement of oxygen atoms, and ρ is the atomic density of SiO_2. Using Eqs. (1) and (2), the SiO_2 atomic density, ρ, is simply given by

$$C\rho = \nu_{LO}^2 - \nu_{TO}^2, \tag{3}$$

where *C* is a constant. Using the values for thick thermal SiO_2 layers, i.e., ν_{TO} of 1090 cm^{-1}, ν_{LO} of 1256 cm^{-1}, and ρ of 2.28×10^{22} /cm^3 [20], and assuming that the shift in ν_{TO} caused by the geometrical effect [20] is 5 cm^{-1} between the thin NAOS SiO_2 layers employed in the present study and thick SiO_2 layers, the atomic density of the SiO_2layers formed by the immersion of Si in 40 wt % HNO_3 is estimated to be 2.19×10^{22}/cm^2 (spectrum a), which is $\sim$4 % lower than that of thick thermal SiO_2 layers. We think that nano-size pores are present in the SiO_2layers, and the decomposition of HNO_3 proceeds at the pore surfaces. It is also likely that diffusion of oxidizing species, i.e., oxygen atoms formed by the decomposition of HNO_3 [9], is enhanced by the presence of nano-size pores. The subsequent immersion in the 68 wt % HNO_3 increases the atomic density to 2.22×10^{22}/cm^2. The SiO_2 layers formed in 68 wt % HNO_3 from the first, on the other hand, have a high atomic density of 2.34×10^{22}/cm^2, which is $\sim$3 % higher than that of thick thermal SiO_2 layers. It is likely that the high atomic density SiO_2 layers retard the diffusion of oxidizing species, resulting in the saturation of the SiO_2 thickness at 1.4 nm.

Figure 3 shows I-V curves for the <Al/3.5 nm SiO_2/Si(100)> MOS diodes with the SiO_2 layer formed by the two-step NAOS method. In the case of deposited 3.5 nm layers formed by

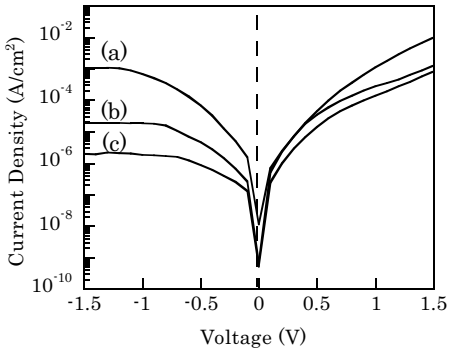

Fig. 3. I-V curves for the <Al/3.5 nm SiO_2/Si(100)> MOS diodes with the SiO_2 layer formed with the two-step NAOS method; a) with no PMA; b) with PMA at 200 °C in hydrogen; c) with PMA at 250 °C in hydrogen.

a CVD method using TEOS, I-V curves could not be measured because of high leakage current densities, indicating a direct contact between Al and Si caused by nonuniform SiO_2 thickness. In the case of the NAOS SiO_2 layers, the I-V curves could be measured even with no treatment (curve a), showing the formation of uniform SiO_2 layers. The leakage current density was decreased by PMA at 200 °C (curve b), and further reduced by PMA at 250 °C (curve c).

Figure 4 shows C-V curves for the same MOS diodes employed in Fig. 3. For the as-formed NAOS SiO_2 layers, a hysteresis with the magnitude of $\sim$0.3 V and a shoulder peak were present in the C-V curve (curve a), attributable to slow states and interface states, respectively [21]. With PMA at 200 °C, the shoulder peak disappeared but the hysteresis was still present with the reduced magnitude of $\sim$0.15 V (curve b). When the PMA temperature was increased to 250 °C, the hysteresis was eliminated almost completely (curve c). Considering these results, we conclude that the decrease in the leakage current density by PMA was mainly due to the elimination of interface states and slow states.

For the formation of thicker SiO_2 layers, we have investigated the bias-assisted NAOS method as described below: Figure 5 shows the thickness of the SiO_2 layers formed by the bias-assisted NAOS method vs. the oxidation time in 1 M HNO_3 at 25 °C. When 5 V was applied to Si during the immersion (plot a), the SiO_2 thickness increased up to 30 min and then remained constant at $\sim$6 nm. It is likely that when the SiO_2 thickness reached $\sim$6 nm, oxidizing species could not reach the SiO_2/Si interface. In the case of the bias voltage at 10 V (plot b), on the other hand, the SiO_2 thickness increased to at least 13 nm. In the case of the bias voltage at 20 V (plot c), the SiO_2 thickness increased almost linearly with the oxidation time at least up to 22 nm. The linear plot probably resulted from the enhancement of the migration of oxidizing species by the electrical field induced in SiO_2 by biasing, leading to in the interfacial reaction-limited mechanism [22]. The enhancement of the inward movement by the positive bias indicates that the oxidizing species is anions. The occurrence of the room-temperature oxidation shows that the oxidizing species possesses great oxidizing ability. Therefore, dissociated oxygen ions (O^-) are the most probable oxidizing species. O^- has a positive electron affinity of 1.47 eV [23], while

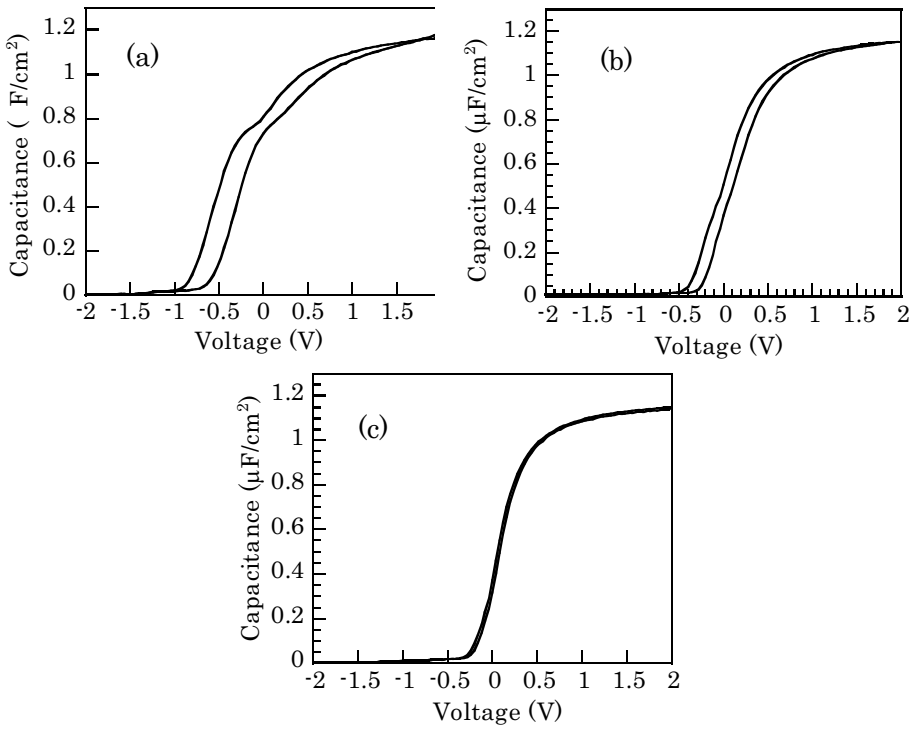

Fig. 4. C-V curves for the <Al/3.5 nm SiO_2/Si(100)> MOS diodes with the SiO_2 layer formed with the two-step NAOS method; a) with no PMA; b) with PMA at 200 °C in hydrogen; c) with PMA at 250 °C in hydrogen.

that of O^{2-} is negative (-7.27 eV) [23], and thus the formation of O^{2-} is unlikely. The oxidation mechanism due to O^- ions is similar to that of platinum-enhanced oxidation of Si where O^- ions are formed by the catalytic activity of platinum [24, 25]. In the case of anodic oxidation of Si where a high bias voltage ranging 30 ∼200 V is applied to Si [26–28], oxidation proceeds at surfaces, not at interfaces [29]. Therefore, the initial Si surface becomes the SiO_2/Si interface after anodic oxidation, resulting in the poor interface characteristics. In the case of the bias-assisted NAOS method, on the other hand, the reaction proceeds at the SiO_2/Si interface, and thus the interface is always clean, leading to relatively good interface characteristics.

Figure 6 shows the I-V curves for <Al/8 nm SiO_2/Si (100)> MOS diodes with the SiO_2 layer formed by the immersion in the 1 M HNO_3 aqueous solutions for 1 h with the bias voltage of 10 V. Even with no heat treatment (curve a), the leakage current density was not high (e.g., 1×10^{-7} at V_G = 5 V). The density of the leakage current markedly decreased (e.g., 4×10^{-10} A/cm^2 at V_G = 5 V) by POA at 600 °C (curve c).

Figure 7 shows the C-V curves for <Al/SiO_2/Si (100)> MOS diodes with the SiO_2 layers formed in the 1 M HNO_3 aqueous solution with the bias voltage of 10 V. With no treatment

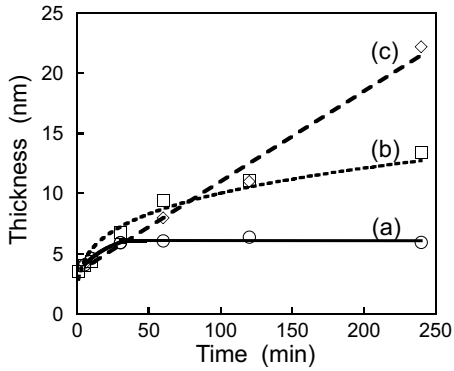

Fig. 5. Thickness of the SiO_2 layers formed in 1 M HNO_3 solutions at 25 °C with the following bias voltages applied to Si with respect to the reference Pt electrode as a function of the immersion time: a) 5 V; b) 10 V; c) 20 V.

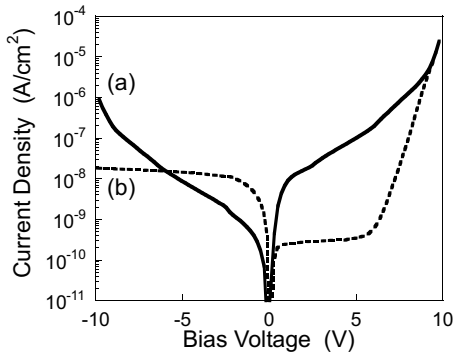

Fig. 6. I-V curves for <Al/SiO_2/Si (100)> MOS diodes with the SiO_2 layer formed in the 1 M HNO_3 solution with the bias voltage of 10 V: a) without POA; b) with POA at 600 °C in nitrogen.

(curve a), a hysteresis with the large magnitude of 1.6 V was observed. The direction of the hysteresis shows that it is due to slow states but not due mobile ions [21]. With POA at 600 °C in nitrogen (curve b), the magnitude of the hysteresis was greatly decreased to ∼0.2 V. Therefore, the decrease in the leakage current density by POA is most probably due to the elimination of slow states.

The relative dielectric constant, ε_{ox} , of the SiO_2layers can be estimated from the SiO_2 thickness, d_{ox}, estimated from XPS or ellipsometry measurements and the SiO_2capacitance, C_{ox}, using the following equation

$$\varepsilon_{ox} = \frac{C_{ox} d_{ox}}{\varepsilon_{_V}}, \tag{4}$$

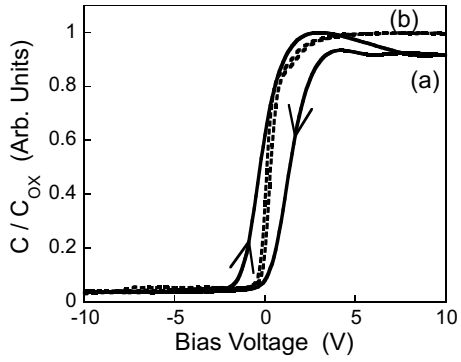

Fig. 7. C-V curves for <Al/SiO_2/Si(100)> MOS diodes with the SiO_2 layer formed in the 1 M HNO_3 solution with the bias voltage of 10 V: a) without POA; b) with POA at 600 °C in nitrogen.

where ε_V is the vacuum permittivity. Ellipsometry measurements show that the SiO_2 thickness is nearly unchanged by POA in nitrogen while the SiO_2 capacitance increases with the POA temperature. Using Eq. (4), ε_{ox} of the SiO_2 layers without and with POA at 600 °C in nitrogen is estimated to be 5.7 and 4.0, respectively. In our previous study, we observed that water molecules desorb from SiO_2 at ∼200 °C while a part of silanol groups desorb around 600 °C and the complete removal requires higher temperature (∼800 °C) [8]. Water molecules and silanol groups are the highly polarized species and thus ε_{ox} is increased by the inclusion of these species. Therefore, the decrease in ε_{ox} by POA is attributable to desorption of water and silanol group. After POA at 600 °C, becomes nearly the same as that of bulk SiO_2 of 3.9, indicating the desorption of all highly polarized species.

The C-V measurements show that slow states are eliminated by POA. The slow states may be due to water molecules included in the NAOS SiO_2 layers. Majority carriers can flow through SiO_2 by hopping the slow states (i.e., trap-assisted tunneling [30]). The decrease in the leakage current density by POA (Fig. 6b) is likely to result from the elimination of the slow states. The slow states are likely to be present away from the SiO_2/Si interface and thus they are more easily removed than fast states which are located close to or at the interface.

4 Conclusion

We have developed a method of the formation of relatively thick SiO_2 layers by use of nitric acid, i.e., two-step NAOS method and bias-assisted NAOS method. For the two-step NAOS method, a ∼1 nm thick SiO_2 layer is initially formed by the immersion in the 40 wt % HNO_3 aqueous solution and then the specimens is immersed in the 68 wt % HNO_3 solution. The 3.5 nm thick NAOS SiO_2 layer thus formed has a relatively low leakage current density (e.g., 1×10^{-2} A/cm^2 at V_G = 1.5 V). With PMA at 250 °C in hydrogen, the leakage current density markedly decreases (e.g., 8×10^{-4}A/cm^2 at V_G = 1.5 V), and the reduction is attributable to the elimination of interface states and slow states. Relatively thick (i.e., ∼10 nm) SiO_2 layers can be formed by the bias-assisted NAOS method. Even without heat treatment, the leakage current density is

relatively low (e.g., 4×10^{-8} A/cm^2 at V_G = 5 V) and it is further decreased by POA at 600 °C in nitrogen, resulting in the low leakage current density of 4×10^{-10} A/cm^2 at V_G = 5 V. The decrease by POA is attributed to the elimination of slow states in SiO_2.

References

[1] Y. Nishi, T. Funai, H. Izawa, T. Fujimoto, H. Morimoto, M. Ishii: *Jpn. J. Appl. Phys. Part 1* **31** (1992) 4570

[2] K. M. Chang, W. C. Yang, C. P. Tsai: *IEEE Electron Device Lett.* **24** (2003) 512

[3] M. Meitine, A. Sazonov: *Proceeding of Materials Research Society Symposium* **769** (2003) 165

[4] A. Kumagai, K. Ishibashi, G. Xu, M. Tanaka, H. Nogami, O. Okada: *Vacuum* **66** (2002) 317

[5] H.U. Kim, S.-W. Rhee: *J. Electrochem. Soc.* **147** (2000) 1473

[6] Asuha. T. Kobayashi, O. Maida, M. Inoue, M. Takahashi, Y. Todokoro, H. Kobayashi: *Appl. Phys. Lett.* **81** (2002) 3410

[7] Asuha, Y. Yuasa, O. Maida, H. Kobayashi: *Appl. Phys. Lett.* **80** (2002) 4175

[8] Asuha, M. Takahashi, H. Kobayashi: *Surf. Sci.* **547** (2003) 275

[9] H. Kobayashi, Asuha, M. Takahashi, H. Iwasa: *J. Appl. Phys.* **94** (2003) 7328

[10] Asuha, Y.-L. Liu, O. Maida, M. Takahashi, H. Kobayashi: *J. Electrochem. Soc.* **151** (2004) G824

[11] H. S. Momose, M. Ono, Y. Yoshitomi, T. Ohguro, S. Nakamura, M. Saito, H. Iwai: *IEEE Trans. Electron. Device* **43** (1996) 1233

[12] S.-H. Lo, D. A. Buchanan, Y. Taur, W. Wang: *IEEE Electron Device Lett.* **18** (1997) 209

[13] J. Joseph, Y. Z. Hu, E. A. Irene: *J. Vac. Sci. Technol. B* **10** (1992) 611

[14] W. Kern, D. A. Puotinen: *R.C.A. Rev.* **31** (1970) 187

[15] F. J. Himpsel, F. R. McFeely, A. Taleb-Ibrahimi, J. A. Yarmoff, G. Hollinger: *Phys. Rev. B* **38** (1998) 6084

[16] H. Kobayashi, T. Yuasa, Y. Niakato, K. Yoneda, Y. Todokoro: *J. Appl. Phys.* **80** (1996) 4124

[17] A. Lehman, L. Schuman, K. Hübner: *Phys. Status Solidi B* **117** (1983) 689

[18] K. T. Queeney, M. K. Weldon, J. P. Chang, Y. J. Chabal, A. B. Gurevich, J. Sapjeta, R. L. Opila: *J. Appl. Phys.* **87** (2000) 1322

[19] K. Ishikawa, H. Ogawa, S. Fujimura: *J. Appl. Phys.* **85** (1999) 4076.

[20] C. Martinet, R. A. B. Devine: *J. Appl. Phys.* **77** (1995) 4343

[21] E. H.Nicollian, J. R. Brews: *MOS (Metal Oxide Semiconductor) Physics and Technology*, Wiley, New York, 1982

[22] S. M. Sze: *VLSI Technology*, McGram-Hill, 1984, Chap. 4

[23] F. A. Cotton, G. Wilkinson, P. L. Gaus: *Basic Inorganic Chemistry*, 3$^{\mathrm{rd}}$ ed., Wiley, New York, 1995

[24] H. Kobayashi, T. Yuasa, Y. Nakato, K. Yoneda, Y. Todokoro: *J. Appl. Phys.* **80** (1996) 4124

[25] H. Kobayashi, T. Yuasa, K. Yamanaka, K. Yoneda, Y. Todokoro: *J. Chem. Phys.* **109** (1998) 4997

[26] V. P. Parkhutik: *Electrochim. Acta* **36** (1981) 1611

[27] K. B. Klark, J. A. Bardwell, J. M. Baribeau: *J. Appl. Phys.* **765** (1994) 3114

[28] C. F. Yeh, J. S. Liu, M. C. Chiang: *Microelectro. Eng.* **48** (1999) 235

[29] P. F. Schmidt, A. E. Owen: *J. Electrochem. Soc.* **111** (1964) 682

[30] A. R. Riben, D. L. Feucht: *Int. J. Electron.* **20** (1966) 583